# On the formation and morphology of lipid nanoparticles containing Ionizable cationic lipids and siRNA

ACS NANO
Cite This: ACS Nano XXXX, XXX, XXX−XXX
www.acsnano.org
ARTICLE

# Formation and Morphology of Lipid Nanoparticles Containing Ionizable Cationic Lipids and siRNA

Jayesh A. Kulkarni,[†] Maria M. Darjuan,[†] Joanne E. Mercer,[‡] Sam Chen,[†,§] Roy van der Meel,[†,∥] Jenifer L. Thewalt,[‡] Yuen Yi C. Tam,[†,§] and Pieter R. Cullis*[,†,⊥]

[†]Department of Biochemistry and Molecular Biology, University of British Columbia, 2350 Health Sciences Mall, Vancouver, British Columbia V6T 1Z3, Canada

[‡]Department of Physics, Simon Fraser University, 8888 University Drive, Burnaby, British Columbia V5A 1S6, Canada

[§]Integrated Nanotherapeutics, 2350 Health Sciences Mall, Vancouver, British Columbia V6T 1Z3, Canada

[∥]Department of Clinical Chemistry and Haematology, University Medical Center Utrecht, 3584 CX Utrecht, The Netherlands

Supporting Information

**ABSTRACT:** **Lipid nanoparticles (LNPs) containing short interfering RNA (LNP-siRNA) and optimized ionizable cationic lipids are now clinically validated systems for silencing disease-causing genes in hepatocytes following intravenous administration. However, the mechanism of formation and certain structural features of LNP-siRNA remain obscure. These systems are formed from lipid mixtures (cationic lipid, distearoylphosphatidylcholine, cholesterol, and PEG-lipid) dissolved in ethanol that is rapidly mixed with siRNA in aqueous buffer at a pH (pH 4) where the ionizable lipid is positively charged. The resulting dispersion is then dialyzed against a normal saline buffer to remove residual ethanol and raise the pH to 7.4 (above the p$K_a$ of the cationic lipid) to produce the finished LNP-siRNA systems. Here we provide cryogenic transmission electron microscopy (cryo-TEM) and X-ray evidence that the complexes formed between siRNA and ionizable lipid at pH 4 correspond to tightly packed bilayer structures with siRNA sandwiched between closely apposed monolayers. Further, it is shown that ionizable lipid not complexed to siRNA promotes formation of very small vesicular structures at pH 4 that coalesce to form larger LNP structures with amorphous electron dense cores at pH 7.4. A mechanism of formation of LNP-siRNA systems is proposed whereby siRNA is first sandwiched between closely apposed lipid monolayers at pH 4 and subsequently trapped in these structures as the pH is raised to 7.4, whereas ionizable lipid not interacting with siRNA moves from bilayer structure to adopt an amorphous oil phase located in the center of the LNP as the pH is raised. This model is discussed in terms of previous hypotheses and potential relevance to the design of LNP-siRNA systems.**

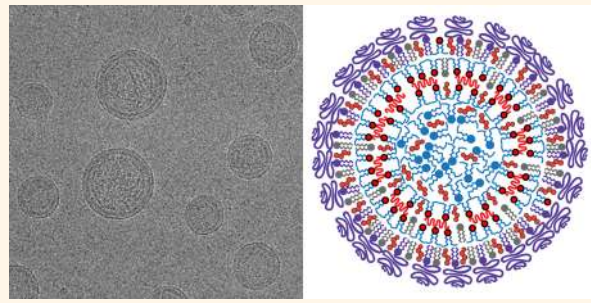

**KEYWORDS:** *lipid nanoparticles, gene therapy, lipid biophysics, cryo-TEM, nanomedicine*

In recent years the mantra surrounding gene therapy has been "delivery, delivery, delivery",[1−3] meaning that intracellular delivery of macromolecular RNA and DNA constructs into target cells was the primary impediment to practicing gene therapy *in vivo*. Viral vectors suffer from immunogenicity, manufacturing, and other concerns, whereas nonviral vectors have toxicity and potency issues. However, the recent successful Phase III trial of a lipid nanoparticle (LNP) formulation of siRNA to treat transthyretin (TTR)-induced amyloidosis suggests that nonviral vectors are starting to overcome the delivery barrier.[4] A key advance has been identification and incorporation of an optimized ionizable cationic lipid in the LNP-siRNA systems. Examples of such lipids are heptatriaconta-6,9,28,31-tetraen-19-yl 4-(dimethylamino)butanoate (DLin-MC3-DMA or MC3) and 2,2-dilinoleyl-4-(2-dimethylaminoethyl)-[1,3]-dioxolane (DLin-KC2-DMA or KC2).[5,6] These lipids exhibit acid-dissociation constants (p$K_a$) below 7, ensuring a near neutral surface charge in the circulation upon intravenous administration, yet a strong positive charge at acidic pH to allow entrapment of nucleic acid polymers. Lipids such as MC3 and KC2 have been optimized for *in vivo* gene silencing in hepatocytes following intravenous (i.v.) administration and exhibit p$K_a$ values in the range 6.2−6.7.[5]

Received: February 26, 2018
Accepted: April 3, 2018
Published: April 3, 2018




DOI: 10.1021/acsnano.8b01516
ACS Nano XXXX, XXX, XXX−XXX

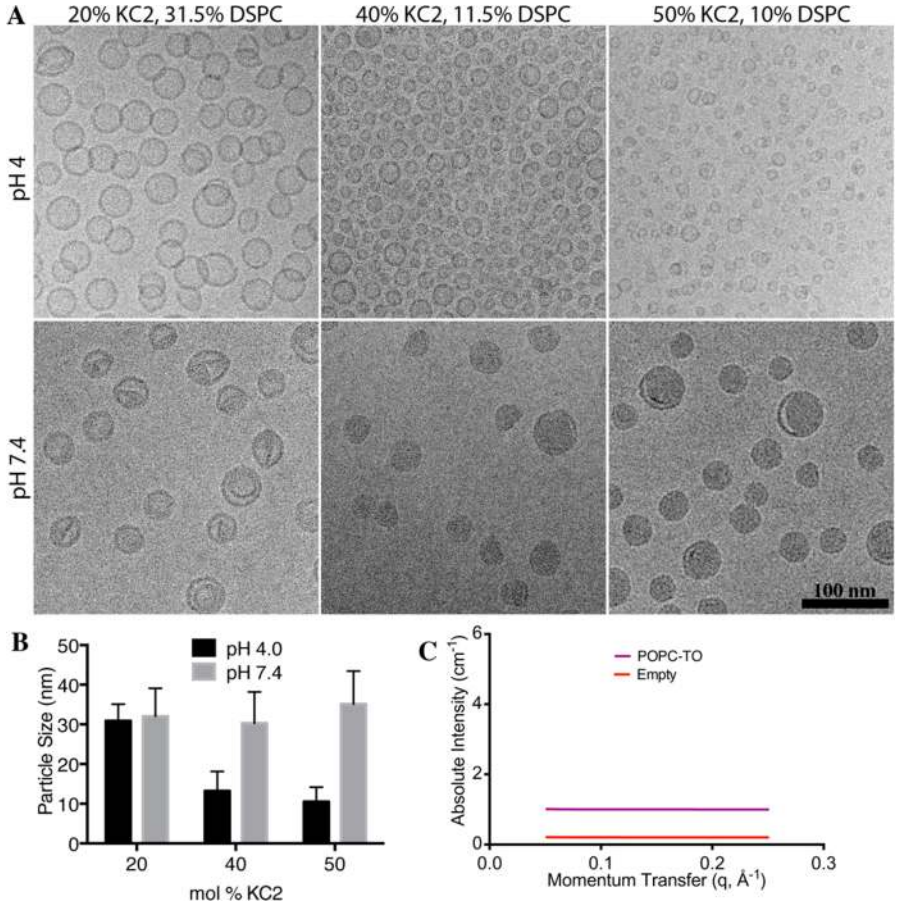


**Figure 1. LNPs prepared in the absence of siRNA exhibit lamellar, vesicular structure at pH 4 and lamellar-solid core structures at pH 7.4, where the proportion of solid core increases as the KC2 content increases. LNPs composed of KC2, DSPC, Chol, PEG-lipid at a molar composition of 20−50/10−31.5/38.5−47.5/1.0−1.5,respectively, were formulated in the absence of siRNA. (A) Cryo-TEM was performed following dialysis to remove ethanol (pH 4), or dialysis against PBS to raise the pH and neutralize the KC2 (pH 7.4). Scale bar = 100 nm. (B) Particle sizing data for the respective formulations at pH 4 and pH 7.4. Results indicate mean ± s.d. (C) SAXS data for POPC/triolein/PEG-lipid LNPs (27/72/1 mol %) and "empty" LNPs composed of KC2/DSPC/cholesterol/PEG-lipid (50/10/38.5/1.5 mol %). In order to accommodate the SAXS data, each set was given an offset (Empty: 0.2, and POPC-TO: 1 units).**

The physical processes by which these lipids enable entrapment and intracellular delivery of negatively charged polymers, and the structures formed, remain poorly characterized. LNP-siRNA systems are generated by rapid mixing of lipids in ethanol with siRNA in aqueous buffer (pH 4.0), followed by dialysis to remove ethanol and to raise the pH to 7.4.[7] The resulting structures display an electron-dense core as observed by cryo-TEM.[8] We have suggested that this core structure is generated through the initial association of ionizable cationic lipid with siRNA to form inverted micellar structures, followed by association with "empty" inverted micelles (formed from excess ionizable lipid) to form a hydrophobic core which is subsequently coated with more polar lipids (DSPC, PEG-lipids) as the polarity is increased.[2,7−10] However, this hypothesis does not account for certain features such as the fact that LNP-siRNA suspensions formed by rapid-mixing methods are initially transparent at pH 4 (indicating the presence of structures smaller than 30 nm diameter) and only become translucent upon dialysis, indicating the presence of larger structures. Moreover, alternative hypotheses of LNP structure[11] also do not necessarily consider these observations or reconcile all of the collected data.

Here, we re-examine the mechanism of LNP formation and the nature of the electron-dense structures formed using cryo-TEM and small-angle X-ray approaches. We show that LNP-siRNA formed using ethanol dilution/rapid-mixing techniques displays a small multilamellar structure at high siRNA contents, where the nucleic acid is trapped between closely apposed lipid bilayers. At lower (clinically relevant) siRNA contents, LNP-siRNA systems exhibit a combination of siRNA-bilayer structure and an amorphous electron dense core, likely arising from an oil droplet consisting primarily of the neutral form of the ionizable cationic lipid.

## RESULTS AND DISCUSSION

**LNP Systems Containing KC2 Adopt Bilayer Structure at pH 4 and Amorphous "Solid Core" Structures at pH 7.4.** Initial experiments focused on characterizing the morphology of LNP systems containing KC2 formulated in the absence of siRNA. When formulated using rapid mixing methods,[7,8,12,13] LNPs formed from lipid mixtures consisting of KC2, DSPC, cholesterol, and PEG-lipid (20−50/10−31.5/39−47.5/1.0−1.5 mol %) at pH 4 display bilayer vesicular structures (Figure 1A) ,where the size decreased as the KC2 content increased (Figure 1B). LNPs formed with 20 mol % KC2 exhibited a diameter of 30 ± 8 nm, whereas LNPs containing 50 mol % KC2 had a diameter of 11 ± 4 nm. When these formulations were dialyzed against phosphate-buffered saline (PBS) to bring the pH to 7.4, a progressive transformation to an electron-dense amorphous core


DOI: 10.1021/acsnano.8b01516
ACS Nano XXXX, XXX, XXX−XXX

structure was observed as the KC2 content increased to 50 mol %. The observation that ionizable cationic lipids transform from small vesicular structures at pH 4.0 into much larger electron-dense core structures as the pH is neutralized suggests large-scale fusion of the small vesicles as the ionizable lipids adopt a neutral form. For the LNP systems containing 50 mol % KC2 (diameter 10.5 nm at pH 4, 35.1 nm at pH 7.4, see Figure 1B), assuming the cross-sectional surface area of a charged ionizable lipid is 0.7 $nm^2$, a lipid density of 0.9 g/mL, and a molecular weight of 590 g/mol, the "solid core" particles observed at pH 7.4 reflect fusion of some 36 vesicles observed at pH 4.

The solid core structure likely reflects an oil droplet phase formed from the neutral ionizable lipid as free-base KC2 adopts a liquid oil phase at room temperature. Previous work[14] using the rapid-mixing formulation process has shown that oil-in-water emulsions composed of POPC and triolein form "limit-size" solid core structures with similar morphology as the LNP systems containing 40 mol % KC2 at pH 7.4. The size of the POPC-triolein LNP increases as the core (triolein) to surface (POPC) lipid ratio is raised.[14,15] Similar behavior is observed for the KC2-containing LNP at pH 7.4. As shown in Supporting Figure 1, as the proportion of KC2 is raised from 40 mol % to 90 mol %, the LNPs (pH 7.4) increase in size from 30 to 90 nm, consistent with an increase in core lipid to surface (PEG-lipid, DSPC) lipid. Interestingly, small-angle X-ray scattering (SAXS) data of empty LNPs composed of KC2/DSPC/cholesterol/PEG-lipid (50/10/38.5/1.5 mol %) showed a similar scattering profile as POPC-triolein LNPs (Figure 1C), suggesting that no structured features are found within the nanoparticle.

Factors that could influence the structure of the amorphous core lipid structures observed at pH 7.4 include the unsaturation of the acyl chains of the ionizable cationic lipid and the charge on the cationic lipid. Increased unsaturation of the acyl chains has been shown to lead to higher levels of transfection[16] and increased propensity for formation of electron-dense core structure.[10] In order to determine whether reducing acyl chain unsaturation affected LNP structure, DODMA, which contains one unsaturated bond per acyl chain compared to two for KC2, was employed. LNPs were formulated with DODMA/DSPC/Chol/PEG-lipid over the range 20–40 mol % DODMA. As shown in Supporting Figure 2 broadly similar morphology was observed as for the KC2-containing systems, although it should be noted that DODMA has a higher apparent $pK_a$ than KC2,[16] and thus at pH 7.4 is deprotonated to a lesser extent than KC2.

The lipid composition of the amorphous core structure is of interest. The dominant component is clearly KC2 as the proportion of the LNP adopting the core structure increases as the KC2 content increases (Figure 1A). The question is whether it is purely KC2 or whether other lipid components are present. Computer modeling places the PEG-lipid on the LNP surface[8] as does the direct influence of PEG-content on LNP size.[7,8,17] DSPC is likely preferentially located in the LNP surface monolayer as well given its amphipathic structure and is unlikely to be significantly soluble in a KC2 oil phase given the insolubility of diglycerides and triglycerides in bilayer membranes.[18] However, the solubility of cholesterol in a KC2 oil phase is not known and was therefore measured as indicated in Supporting Figure 3, leading to the finding that cholesterol has limited solubility in KC2. A solution of KC2 saturated with cholesterol at room temperature contains approximately 8 mol % of cholesterol. The amorphous core structure is therefore ascribed to the neutral form of KC2 containing a small amount of cholesterol.

**LNP Systems Containing Permanently Cationic Lipids Do Not Exhibit Solid Core Structure.** In order to demonstrate that the amorphous core is consistent with the presence of KC2 in the neutral form, the morphology of LNP formed when DOTMA (a permanently positively charged analogue of DODMA) was substituted for KC2, was investigated. As shown in Figure 2A, the behavior of LNP containing DOTMA at pH 4

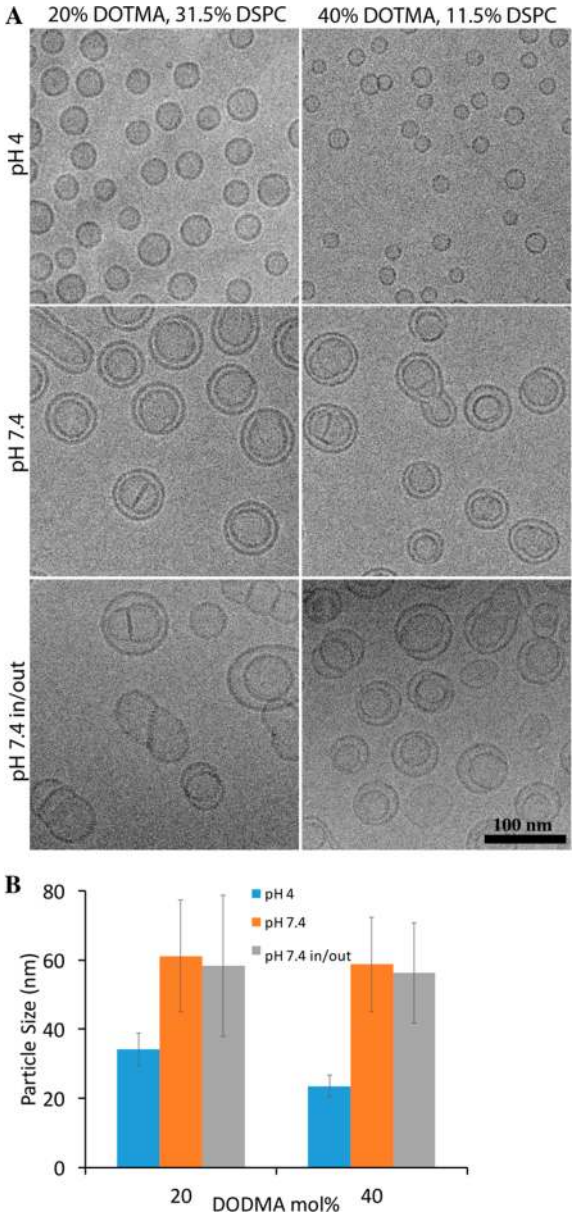


**Figure 2. LNPs containing permanently positively charged lipid do not exhibit electron-dense core structure. LNPs composed of DOTMA, DSPC, Chol, PEG-DSPE at a molar composition of 20–40/11.5–31.5/47.5/1.0, respectively, were formulated in the absence of siRNA. (A) Cryo-TEM was performed following dialysis to remove solvent (while still at pH 4), or to neutralize the pH (PBS pH 7.4). Another set of formulations was generated in PBS pH 7.4 and dialyzed into PBS pH 7.4 to remove ethanol (labeled pH 7.4 in/out). Scale bar = 100 nm. (B) Particle sizing data for the respective formulations at pH 4 and pH 7.4. Results indicate mean ± s.d.**

was similar to that observed for KC2-containing LNP, with smaller vesicular structures observed as the DOTMA content was raised from 20 to 40 mol %. The morphology observed on



DOI: 10.1021/acsnano.8b01516
ACS Nano XXXX, XXX, XXX–XXX

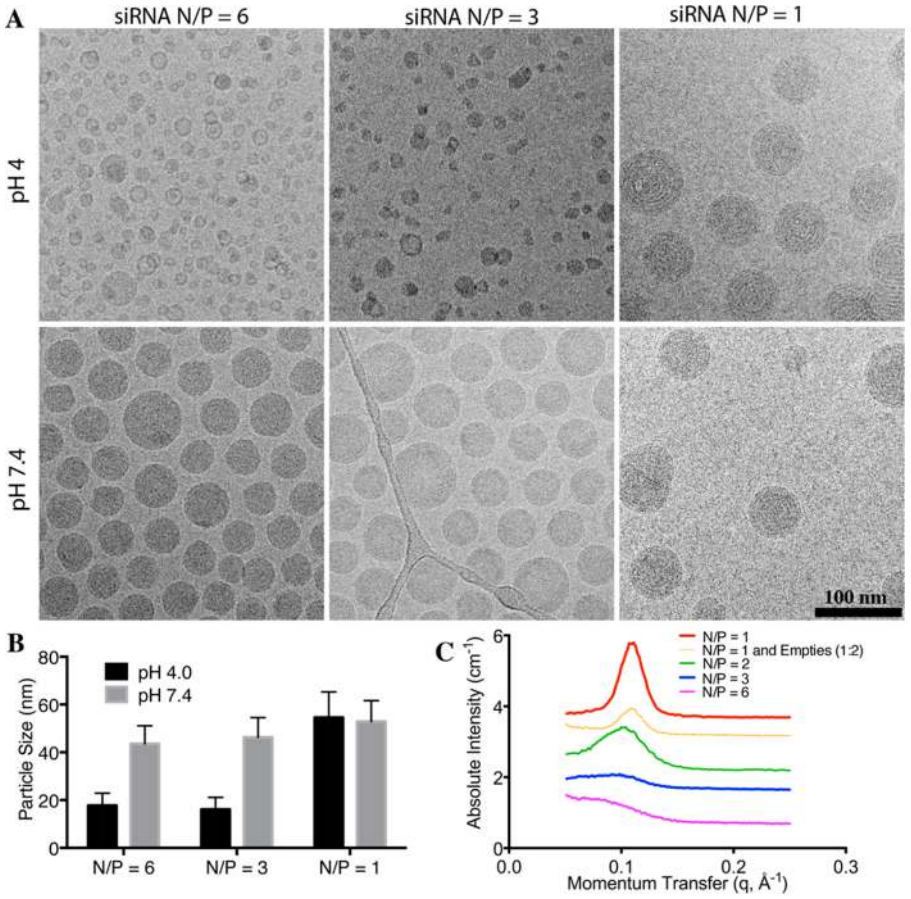


**Figure 3. LNP prepared in the presence of siRNA exhibit stacked bilayer structure at high siRNA contents, where the proportion of stacked structures decreases as the siRNA content decreases. LNPs composed of KC2, DSPC, Chol, PEG-lipid at a molar composition of 50/10/38.5/1.5 were formulated at various charge ratios (N/P = 1, 3, or 6). (A) Cryo-TEM was performed following dialysis to remove ethanol (pH 4), or dialysis against PBS to raise the pH and neutralize the KC2. Scale bar = 100 nm. (B) Particle sizing data for the respective formulations at pH 4 and pH 7.4. Results indicate mean ± s.d. (C) Small-angle X-ray scattering data for LNP-siRNA formulations at pH 7.4. Formulations were generated at N/P = 1−6. A mixture of LNP-siRNA (N/P = 1) and empty LNPs was also analyzed. LNP-siRNA at N/P = 1 displays a scattering pattern characteristic of a bilayer structure closely supporting the cryo-TEM data. For the full scattering pattern ($q$ = 0.012−0.3 Å$^{-1}$), refer to Supporting Figure 5.**

dialysis against PBS pH 7.4 was, however, very different. In all cases a conversion from unilamellar vesicular structures to primarily bilamellar systems and an increase in particle size (Figure 2B) were observed, with no evidence for amorphous electron-dense core structures.

The results of this section lead to three conclusions. First, and most importantly, the amorphous "solid core" structure associated with LNP systems at pH 7.4 containing ionizable cationic lipids such as KC2 and DODMA at 20 mol % or higher is consistent with formation of oil droplets in the LNP interior consisting of the neutral (deprotonated) form of the ionizable lipid with a small proportion (8 mol %) of cholesterol. The second conclusion is that positively charged ionizable lipids, whether ionizable or permanently positively charged, adopt extremely small vesicular structures (diameter 15 nm or less) when dispersed from ethanol in aqueous buffer by rapid mixing. The reasons for the small size are not clear, but could be due to the relatively small headgroup of these lipids that leads to an inverted cone shape that is more readily accommodated in the inner monolayer of a membrane. A final finding concerns the conversion of unilamellar systems at pH 4 containing 20 mol % cationic lipid (either ionizable or permanently charged) to predominantly bilamellar systems when dialyzed against PBS. This morphological change is clearly not due to the charge on the cationic lipid species, as it is observed for both ionizable and permanently positively charged lipids. In an attempt to determine whether the change in osmotic strength going from 25 mM at pH 4 to 160 mM in PBS could be driving the structural change, LNPs formed from DSPC/Cholesterol/PEG-lipid (55/44/1 mol %) were characterized. As shown in Supporting Figure 4a transition from unilamellar to bilamellar systems was observed for all cases where the exterior medium was of significantly higher osmolarity. The change in morphology appears to arise due to a fusion event and not deformation of vesicles due to osmotic effects, as the LNPs achieved following exposure to media of higher osmolarity are uniformly bigger than the initial structures.

**LNP Systems Containing siRNA Contain a Proportion of Bilayer Structures.** We next proceeded to characterize the influence of encapsulated siRNA on LNP structure. As shown in Figure 3A, at high levels of encapsulated siRNA (amino lipid nitrogen-to-siRNA phosphate (N/P) ratios of 1) where all of the positively charged ionizable lipid is complexed to an RNA phosphate, small multilamellar systems are observed. Such systems (albeit somewhat larger) have been reported previously for LNP containing ionizable cationic lipids and high levels of


DOI: 10.1021/acsnano.8b01516
ACS Nano XXXX, XXX, XXX−XXX

antisense oligonucleotides, where the oligonucleotides reside at the interface between closely apposed bilayers.[19,20] It should be noted that in the present study, the formulations generated at N/P = 1 do not increase in size when the pH is neutralized (Figure 3B), whereas empty formulations or those at N/P = 3 or 6 increase in size when dialyzed into pH 7.4 buffer.

In an attempt to determine whether the LNP-associated siRNA remains complexed in bilayer structures at N/P values of 3 and 6 (where maximum *in vivo* gene silencing activity is realized),[7,17] SAXS studies were performed. As shown in Figure 3C for LNP-siRNA (pH 7.4) systems formulated at an N/P value of 1, scattering curves characteristic of the presence of closely apposed lipid bilayers with a repeat distance of 5.8 nm are observed. It should be noted that previous work[21] has shown that the complexes formed between cationic lipids and plasmid DNA generate lamellar structures with peaks in the range of $q$ = 0.1 Å$^{-1}$. Comparatively, the presence of cubic phases in nanoparticles is observed at low $q$ values (and visualized by cryo-TEM),[22] which is not observed here (Supporting Figure 5). This bilayer signature is also present for LNP-siRNA systems formulated at N/P values of 2, 3, and 6, albeit broadened with a decreased intensity. In order to show that the bilayer signatures at higher N/P values do not arise from a mixture of bilayer siRNA-containing LNP with empty LNP, the SAXS behavior of a mixture of LNP-siRNA systems (at N/P = 1) and empty LNPs at a ratio of 1:2 (w/w) was characterized. As shown in Figure 3C, while the resulting spectrum showed a decreased signal intensity relative to N/P = 1 formulations, there was no peak broadening.

As the siRNA content is reduced to N/P values of 3 and 6, the presence of lamellar structure induced by siRNA as detected by cryo-TEM is less definitive. In order to achieve improved resolution, LNP-siRNA systems were formulated and characterized for N/P values of 1.1 and 1.5, as shown in Figure 4

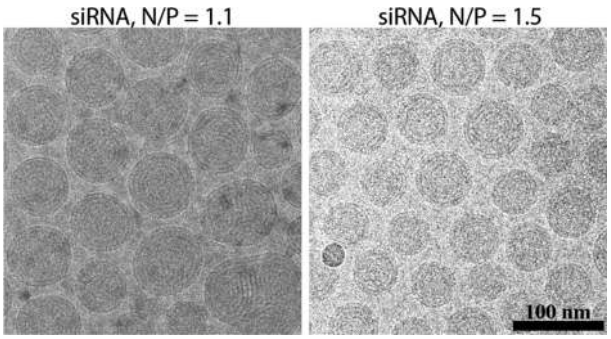


**Figure 4. LNP-siRNA formulations generated at N/P values of 1.1 and 1.5 at pH 7.4 display stacked bilayer structures on the perimeter of the LNP. LNPs composed of KC2/DSPC/Chol/PEG-DMG (50/10/38.5/1.5 mol %) generated with siRNA at N/P = 1.1 and 1.5 were imaged by cryo-TEM. The resulting structures are multilamellar vesicles, with the number of resolved concentric rings decreasing at higher N/P ratios. Scale bar = 100 nm.**

where bilayer structures are observable by cryo-TEM with progressively increased amounts of amorphous structure toward the center of the LNP. It is interesting to note that while siRNA induces bilayer structure (at pH 4) in LNP systems containing very high levels of KC2 and no bilayer forming lipid DSPC, such systems do not maintain bilayer structure at pH 7.4 and release all the associated siRNA as the pH is raised. This is shown in Supporting Figure 6 where, for LNPs composed of 98.5% KC2 and 1.5 mol % PEG-lipid, large stacked bilayer structures are observed at pH 4, while at pH 7.4, amorphous electron-dense structures are seen with no entrapment of siRNA. This observation suggests a need for a certain amount of amphipathic, bilayer-forming lipid such as DSPC to provide the outer monolayer of the LNP-siRNA particle to stabilize the system and maintain internal siRNA-ionizable lipid stacked bilayer structure.

During the later stages of this study, an improved cryo-TEM instrument with higher acceleration voltages (300 kV) and better detection (direct electron detectors rather than CCD) became available. The higher acceleration voltage leads to decreased electron attenuation and improved sample penetration, thus improved imaging of the LNP core. It should be noted that the "solid-core" nature of lipid nanoparticles, as described in previous studies,[7,8,10,17] is influenced by the lower acceleration voltage (200 kV) and the amount of under-focus employed in those studies. Cryo-TEM imaging relies on defocus-enhanced contrast (*i.e.*, contrast is increased at the expense of resolution). Thus, the core of LNP-siRNA, as imaged by a 300 kV instrument, is observed as significantly less electron-dense than when imaged by a 200 kV instrument. The improved resolution possible with the 300 kV instrument clearly reveals that empty LNPs at pH 4 exhibit only bilayer structures, while those containing siRNA (N/P = 3) display lamellar phase within the electron-dense particles (Supporting Figure 7). At pH 7.4, however, the empty LNPs display surface bilayer structure with an amorphous core. Note that this surface bilayer morphology is not observed for LNPs that do not contain DSPC (Figure 5). LNP-siRNA systems with high siRNA contents (N/P ~ 1) exhibit concentric bilayer ring structures consistent with the structures observed using the 200 kV instrument. Slightly higher N/P ratios (1.1–1.5) result in a combination of concentric ring structure and an amorphous core.

In summary, the results of this section indicate that at pH 7.4, LNP-siRNA systems formulated using the ethanol dilution rapid-mixing process consist of siRNA sandwiched between closely apposed bilayer structures preferentially located in outer layers of the LNP and that cationic lipid that is not associated with siRNA adopts amorphous solid core morphology in the center of the LNP-siRNA particle. These data also indicate that the DSPC-lipid preferentially resides on the surface of the LNP.

**Implications for LNP-siRNA Structure and Design.** The results of this investigation demonstrate that at high siRNA contents (N/P = 1), the LNP-siRNA systems formed at both pH 4 and 7.4 adopt a small multilamellar vesicle structure consisting of siRNA sandwiched between closely apposed concentric lipid bilayers. Conversely, LNPs formed in the absence of siRNA at pH 7.4 exhibit an amorphous hydrophobic lipid core consistent with an oil-in-water dispersion. At N/P values of 3 and 6 (which correspond to formulations used clinically) where there is an excess of ionizable cationic lipid, siRNA remains sandwiched within bilayer lipid assemblies (as indicated by small-angle X-ray studies), whereas the LNP core displays amorphous structure consistent with the presence of oil-phase lipid. For systems where there is only a slight excess of ionizable cationic lipid (N/P of 1.5), outer regions of the LNP display concentric ring structure, whereas the LNP center displays amorphous structure. On the basis of these observations we propose a revised model of LNP-siRNA structure for therapeutically active formulations, as shown in Figure 6, where the bulk of the ionizable cationic lipid segregates into a central oil phase and stacked bilayers of lipid-siRNA aggregates are located toward the periphery of the LNP.



DOI: 10.1021/acsnano.8b01516
*ACS Nano* XXXX, XXX, XXX–XXX

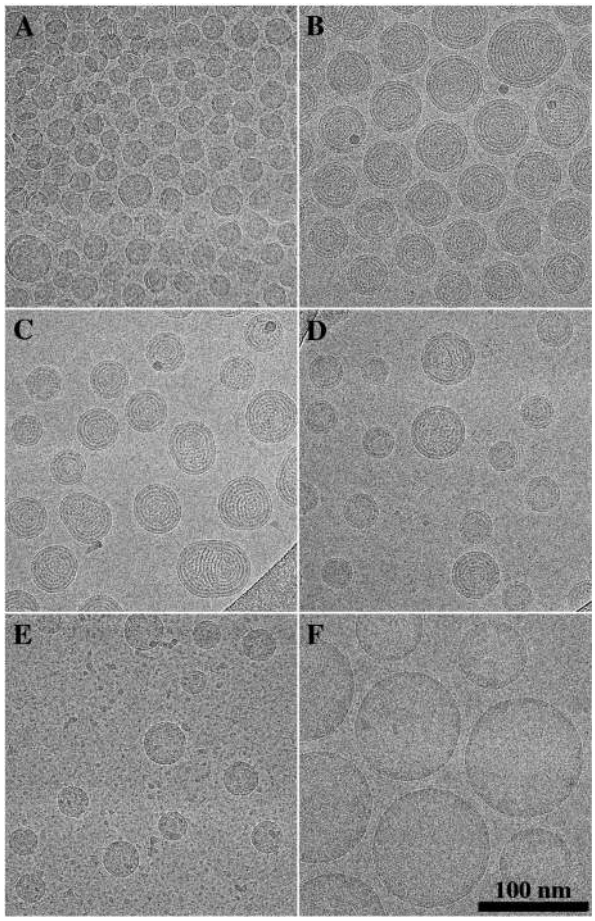


**Figure 5. Cryo-TEM imaging with improved resolution supports the presence of DSPC-lipid on the surface of the LNP. All formulations, at pH 7.4, were vitrified and subjected to cyro-TEM using a 300 kV instrument with direct electron detectors. (A) LNPs composed of KC2/DSPC/cholesterol/PEG-DMG (50/10/38.5/1.5 mol %) generated without siRNA. LNPs of a similar composition were also formulated with siRNA at N/P = 1 (B), 1.1 (C), 1.5 (D), and 6 (E). (F) LNPs composed of KC2/PEG-DMG (98.5/1.5 mol %) were generated without siRNA. Scale bar = 100 nm.**

The structure presented in Figure 6 differs significantly from the structure proposed previously indicating a nanostructured core of LNP-siRNA systems, where siRNA is encapsulated in inverted micelles in the LNP interior in a "currant bun" configuration and excess ionizable cationic lipid that is not complexed to siRNA displays inverted micellar structure.[7,8] This structure was suggested largely by molecular-modeling approaches. All other experimental data presented by Leung *et al.*[8,10] is fully consistent with the model presented here.

The revised structure suggests a number of ways to optimize LNP stability and possibly performance. First, the proportions of DSPC, cholesterol, and ionizable cationic lipids in LNP-siRNA systems have previously been developed through phenomenological approaches to optimize FVII gene silencing potency *in vivo*. The results presented here suggest that optimized ratios derived from these studies should be refined on the basis of the solubility of the lipid components with one another. For example, the optimized ratios for maximum gene silencing potency in hepatocytes in a mouse model are ionizable cationic lipid/DSPC/cholesterol/PEG-lipid (50/10/38.5/1.5 mol %).[5] However, if cholesterol is only 8 mol % soluble in the ionizable lipid oil phase and present at equimolar levels in the DSPC surface monolayer, only 14 mol % of the total cholesterol is accounted for. The remaining 24.5 mol % cholesterol could potentially form crystalline structures and introduce particle instability. Similarly, if DSPC is primarily located in the outer monolayer in equimolar concentrations with cholesterol, an equilibrium size for an LNP containing 10 mol % DSPC would be ~80 nm diameter. Previous work has shown that LNP-siRNA systems containing 10 mol % DSPC exhibit maximum activity for a size of 80 nm diameter.[17] This suggests that to obtain smaller systems with optimized activity, higher levels of DSPC should be incorporated.

It should be noted that while the size of LNP-siRNA systems is controlled by the PEG-lipid content,[7,23] LNP systems that do not contain sufficient DSPC to cover an external surface monolayer will, of necessity, incorporate additional cholesterol and/or ionizable lipid in that monolayer. The PEG-lipid content determines the size of the LNP by virtue of its ability to inhibit further LNP fusion at some critical concentration as the small particles generated at pH 4 coalesce to form the larger LNP observed at pH 7.4. If the particle does not contain sufficient amphipathic lipid to cover the outer surface, it will exist in a metastable state stabilized by the PEG-lipid coat. In the absence of PEG-lipid, further rounds of fusion would be expected to occur until the exterior monolayer contains sufficient amphipathic lipid that additional fusion is inhibited. When the diffusible PEG-lipid dissociates from the LNP following i.v. administration, such nonequilibrium surface lipid compositions may be expected to influence serum protein adsorption to the particle surface, possibly influencing tissue specificity.

## CONCLUSIONS

The major finding of this investigation is that LNP-siRNA systems formed by rapid mixing-ethanol dilution processes do not show evidence of inverted micellar structures containing siRNA dispersed in a "currant bun" pattern in the LNP interior. Rather, the siRNA is associated with closely apposed lipid bilayers sandwiching siRNA molecules that segregate toward the periphery of the LNP. Excess ionizable cationic lipid forms an amorphous lipid core that likely corresponds to an oil-droplet phase that contains a limited amount of cholesterol. These findings suggest that the proportions of different lipid species in optimized LNP-siRNA systems may vary according to the particular ionizable cationic lipid employed. For example, for the KC2 lipid employed here, the limited solubility of cholesterol in the hydrophobic core suggests that the cholesterol content should be reduced to achieve more stable systems. Alternatively, increasing the amount of DSPC may be expected to result in enhanced stability and possibly enhanced activity of smaller LNP systems. Previous work has shown that smaller LNP-siRNA systems are less potent than larger systems.[17]

## MATERIALS AND METHODS

**Materials.** The lipid 1,2-distearoyl-*sn*-glycero-3-phosphorylcholine (DSPC), 1-palmitoyl,2-oleoyl-*sn*-glycero-3-phosphorylcholine (POPC), 1,2-distearoyl-*sn*-glycero-3-phosphoethanolamine-*N*-[methoxy-(polyethylene glycol)-2000] (ammonium salt) (PEG-DSPE), and 1,2-di-*O*-octadecenyl-3-trimethylammonium propane (chloride salt) (DOTMA) were purchased from Avanti Polar Lipids (Alabaster, AL). The ionizable cationic lipid 2,2-dilinoleyl-4-(2-dimethylaminoethyl)-[1,3]-dioxolane (DLin-KC2-DMA) was synthesized by Biofine International (Vancouver, BC). The ionizable cationic lipid 1,2-dioleyloxy-3-dimethylamino-propane (DODMA) was purchased from Cayman Chemical (Ann Arbor, MI). Cholesterol and glyceryl trioleate (triolein) were purchased from Sigma-Aldrich (St. Louis, MO). (*R*)-2,3-bis(tetradecyloxy)propyl-1-(methoxy polyethylene glycol 2000) carbamate (PEG-DMG) was


DOI: 10.1021/acsnano.8b01516
*ACS Nano* XXXX, XXX, XXX−XXX

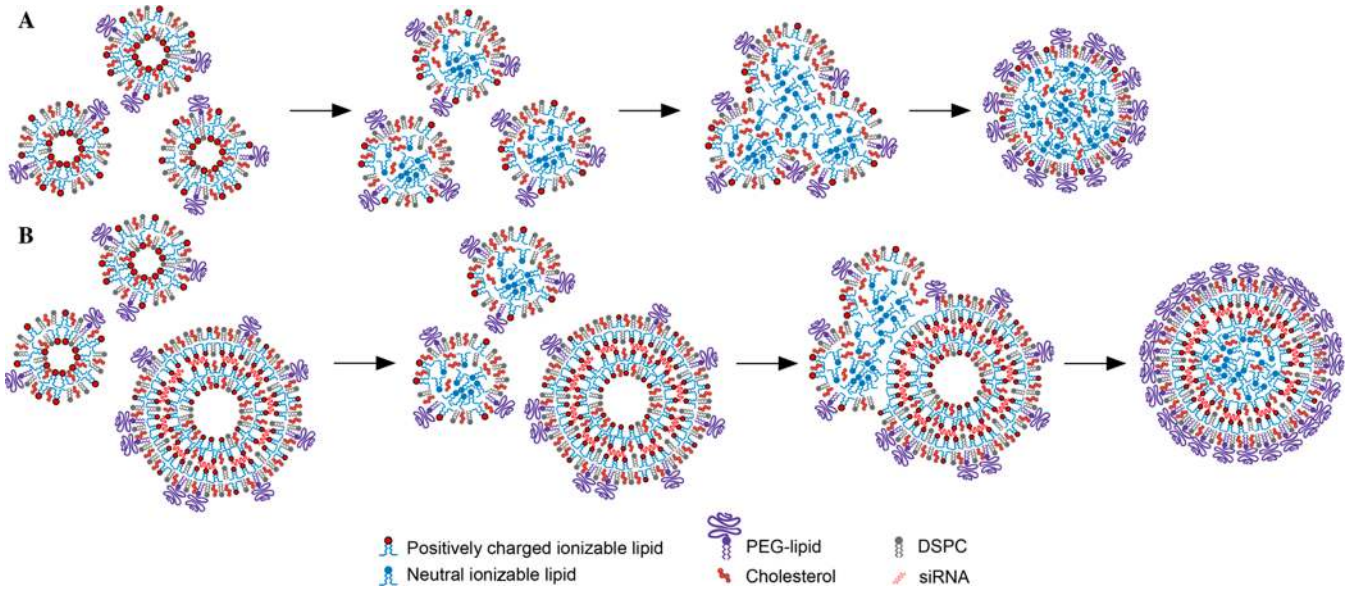


**Figure 6. Proposed mechanism of formation and structure of LNP prepared in the absence and presence of siRNA. (A) In the absence of siRNA, the LNP lipid dispersions form small unilamellar vesicles on rapid mixing at pH 4. As the pH is raised (dialysis against PBS pH 7.4), an increasing proportion of the ionizable cationic lipids adopts a neutral form, thus decreasing intervesicle electrostatic repulsion, destabilizing the bilayer structure, and engendering vesicle fusion. As the vesicles fuse, PEG-lipid, DSPC, and cholesterol (equimolar with DSPC) partition to the outer monolayer of the increasingly large LNP, whereas neutral KC2 partitions to the LNP interior forming an oil droplet phase in the center of the LNP. Equilibrium is achieved when the concentration of PEG-lipid in the outer monolayer is sufficiently high to inhibit further inter-LNP fusion. Note that this equilibrium size may well be considerably smaller than the equilibrium size dictated by the DSPC-cholesterol content. (B) In the presence of siRNA, the initial event is formation of small vesicles which contain siRNA between closely apposed lipid monolayers. As the pH is raised, neutralization of the ionizable lipid induces fusion between various particles similar to the case of empty LNPs. This process is limited by phase separation of PEG-lipid, and possibly DSPC/cholesterol, from the complexes. It is proposed that these lipids are deposited in a surface monolayer that inhibits further fusion. It should be noted that the presence of high levels of ethanol (at least 25% by volume) results in high exchange rates for individual lipid molecules (with the exception of the cationic lipid complexed to siRNA), resulting in rapid formation of equilibrium structures. Note also that the DSPC/cholesterol must sequester, at least in part, to the outer monolayer and stabilize smaller structures at pH 4, as very large micron-size systems are observed for systems containing 1.5 mol % PEG-lipid and no DSPC or cholesterol (see Supporting Figure 5C). As the pH is raised, the situation is much the same as for the LNP in the absence of siRNA; the increasing conversion of the ionizable lipid to the neutral form favors further fusion and deposition in the interior core of the LNP.**

synthesized as previously described.[24] The structures of the lipids used are shown in Supporting Figure 8. TEM grids were purchased from Ted Pella, Inc. (Redding, CA). siRNA against firefly luciferase[25] was purchased from IDT (Coralville, IA).

**Preparation of Empty LNPs.** Previous studies on the morphology of LNP-siRNA systems were conducted with particles generated using a staggered herringbone micromixer (SHM) made of polydimethylsiloxane (PDMS) provided by Precision Nanosystems Inc. (Vancouver, BC).[7,8,10] Here we show both mixing techniques (T-junction mixer[12,13,15] and SHM) generated empty LNPs and LNP-siRNA with similar morphology as observed by cryo-TEM (Supporting Figure 9). Briefly, component lipids (ionizable cationic lipids, DSPC, cholesterol, and PEG-DMG or PEG-DSPE) or emulsion lipids (POPC, triolein) were dissolved in ethanol at appropriate ratios to a final concentration of 15 mM total lipid. The appropriate aqueous and organic solutions were mixed using a T-junction mixer[12,13,15] at a flow rate ratio of 3:1 (v/v; respectively) and a total flow rate of 20 mL/min. The resultant mixture was dialyzed directly against 1000-fold volume of appropriate buffer.

**Preparation of LNPs Containing siRNA.** LNPs containing siRNA were prepared as previously described.[13] Briefly, component lipids (ionizable-amino lipids, DSPC, cholesterol, and PEG-DMG) were dissolved in ethanol at appropriate ratios to a final concentration of 15 mM total lipid. Nucleic acids were dissolved in 25 mM sodium acetate pH 4 buffer. The aqueous and organic solutions were mixed using a T-junction mixer[12,13,15] at a flow rate ratio of 3:1 (v/v; respectively) and a total flow rate of 20 mL/min. The resultant mixture was dialyzed directly against 1000-fold volume of sodium acetate pH 4 buffer or PBS (pH 7.4) overnight.

**Cryogenic Transmission Electron Microscopy.** LNPs were concentrated to a final concentration of 15−25 mg/mL of total lipid. 2−4 $\mu$L of LNP suspension was added to glow-discharged copper grids and plunge-frozen using a FEI Mark IV Vitrobot (FEI, Hillsboro, OR) to generate vitreous ice. Grids were stored in liquid nitrogen until imaged. All samples were imaged with a 200 kV instrument unless otherwise specified.

*For 200 kV Imaging.* Grids were moved into a Gatan 70° cryo-tilt transfer system pre-equilibrated to at least −180 °C and subsequently inserted into the microscope. An FEI LaB6 G2 TEM (FEI, Hillsboro, OR) operating at 200 kV under low-dose conditions was used to image all samples. A bottom-mount FEI Eagle 4K CCD camera was used to capture all images. All samples (unless otherwise stated) were imaged at a 55,000× magnification with a nominal under-focus of 1−2 $\mu$m to enhance contrast. Sample preparation and imaging were performed at the UBC Bioimaging Facility (Vancouver, BC).

*For 300 kV Imaging.* Grids were transferred to an autoloader-equipped FEI Titan Krios (FEI, Hillsboro, OR) operating at 300 kV with a Falcon III direct electron detector. All samples (unless otherwise stated) were imaged at a 47,000× magnification with a nominal under-focus of 1−2 $\mu$m to enhance contrast. Sample imaging was performed at the UBC Life Sciences Centre (Vancouver, BC).

**Analysis of LNPs.** Particle size analysis of LNPs in PBS was carried out using a Malvern Zetasizer (Worcestershire, UK). Cryo-TEM micrographs obtained for each sample were characterized for particle size (as compared by diameter to the scale bar), performed by manual counting of 150 LNPs. Such an approach has been shown to closely correlate with the number-weighted average produced by dynamic light scattering.[8,23] Similarly, morphology of LNPs was quantified manually. Lipid concentrations were measured using the Cholesterol E Total-Cholesterol assay (Wako Diagnostics, Richmond, VA).



DOI: 10.1021/acsnano.8b01516
ACS Nano XXXX, XXX, XXX−XXX

**Solubility of Cholesterol in KC2 oil.** Cholesterol (40 mg) was transferred to a glass vial containing 200 mg of KC2 oil. The vials were then sonicated in a bath sonicator for 60 min at room temperature with intermittent vortex-mixing. The resulting mixture was then centrifuged for 30 min at 17,000×*g* at room temperature. The supernatant was collected, and 10.6 mg was suspended in a 1 mL of isopropanol:methanol (1:1 v/v). The concentration of cholesterol was determined by ultrahigh-pressure liquid chromatography (UPLC) on a Waters Acquity H-Class UPLC System equipped with a BEH C18 column (1.7 $\mu$m, 2.1 Å, ~100 mm) and a photodiode array detector. Separation was achieved at a flow rate of 0.5 mL/min, with a mobile phase consisting of a linear gradient of solvent A (1:1 methanol-acetonitrile mixture) and B (water) from 30:70 to 100:0, respectively, over 6 min at a column temperature of 55 °C. The absorbance at 207 nm was measured, and the cholesterol concentration was determined using calibration curves.

**Small Angle X-ray Scattering.** Small angle X-ray scattering (SAXS) experiments were conducted on the SAXSLAB Ganesha 300XL SAXS system at 4D Laboratories (SFU, Burnaby, BC). The sample to detector distance was adjustable across 1.4 m to allow measurements from $q$ = 0.0025 Å$^{-1}$ to $q$ = 2.8 Å$^{-1}$. The X-ray beam has a wavelength of 0.154 nm generated by a Cu-K$\alpha$ X-ray source. Concentrated LNP suspensions were loaded into quartz capillary tubes purchased from Charles Supper Company (Natick, MA) which are approximately 80 mm long, 1.5 mm in diameter, and 0.01 mm thick. After transfer, the tubes were sealed using capillary wax. Samples were loaded into a temperature-controlled Linkam heater stage which maintained a constant temperature of 22.7 °C throughout all experiments.

## ASSOCIATED CONTENT

### Supporting Information

The Supporting Information is available free of charge on the ACS Publications website at DOI: 10.1021/acsnano.8b01516.

Empty LNP morphology at high KC2 contents, morphology of LNP containing DODMA, quantification of cholesterol solubility in KC2, empty DSPC vesicles in different buffers, SAXS patterns for full $q$ range, LNP morphology with high KC2 and siRNA, cryo-TEM of empty and loaded LNP-siRNA at pH 4 by 300 kV imaging, structures of lipids investigated in the study, and a comparison of T-tube and microfluidic LNP formulation methods (PDF)

## AUTHOR INFORMATION


### Corresponding Author

*E-mail: pieterc@mail.ubc.ca.

### ORCID

Jayesh A. Kulkarni: 0000-0002-3622-6998

Sam Chen: 0000-0002-3738-6600

Jenifer L. Thewalt: 0000-0002-0833-3139

Pieter R. Cullis: 0000-0001-9586-2508

### Present Address

⊥Life Sciences Institute, University of British Columbia, 2350 Health Sciences Mall, Vancouver, British Columbia V6T 1Z3, Canada


### Notes

The authors declare no competing financial interest.

## ACKNOWLEDGMENTS

This work was funded by Foundation grant (FDN 148469) from the Canadian Institutes of Health Research (CIHR), a Strategic Project Grant from the Natural Sciences and Engineering Research Council (NSERC STPGP/463247-2014), and a British Columbia Innovation Council Ignite grant. Dr. Roy van der Meel is supported by a VENI Fellowship (no. 14385) from The Netherlands Organization for Scientific Research (NWO). The authors would like to thank Dr. Miranda Schmidt for technical assistance with the SAXS instrumentation.

## REFERENCES


(1) Kaczmarek, J. C.; Kowalski, P. S.; Anderson, D. G. Advances in the Delivery of Rna Therapeutics: From Concept to Clinical Reality. *Genome Med.* **2017**, *9*, 60.

(2) Cullis, P. R.; Hope, M. J. Lipid Nanoparticle Systems for Enabling Gene Therapies. *Mol. Ther.* **2017**, *25*, 1467.

(3) Elsabahy, M.; Nazarali, A.; Foldvari, M. Non-Viral Nucleic Acid Delivery: Key Challenges and Future Directions. *Curr. Drug Delivery* **2011**, *8*, 235−44.

(4) *Alnylam and Sanofi Report Positive Topline Results from Apollo Phase 3 Study of Patisiran in Hereditary ATTR (hATTR) Amyloidosis Patients with Polyneuropathy*. http://www.businesswire.com/news/home/20170920005628/en/, 2017, accessed Jan 11, 2018.

(5) Jayaraman, M.; Ansell, S. M.; Mui, B. L.; Tam, Y. K.; Chen, J.; Du, X.; Butler, D.; Eltepu, L.; Matsuda, S.; Narayanannair, J. K.; Rajeev, K. G.; Hafez, I. M.; Akinc, A.; Maier, M. A.; Tracy, M. A.; Cullis, P. R.; Madden, T. D.; Manoharan, M.; Hope, M. J. Maximizing the Potency of siRNA Lipid Nanoparticles for Hepatic Gene Silencing *in vivo*. *Angew. Chem., Int. Ed.* **2012**, *51*, 8529−33.

(6) Semple, S. C.; Akinc, A.; Chen, J.; Sandhu, A. P.; Mui, B. L.; Cho, C. K.; Sah, D. W.; Stebbing, D.; Crosley, E. J.; Yaworski, E.; Hafez, I. M.; Dorkin, J. R.; Qin, J.; Lam, K.; Rajeev, K. G.; Wong, K. F.; Jeffs, L. B.; Nechev, L.; Eisenhardt, M. L.; Jayaraman, M.; et al. Rational Design of Cationic Lipids for siRNA Delivery. *Nat. Biotechnol.* **2010**, *28*, 172−6.

(7) Belliveau, N. M.; Huft, J.; Lin, P. J.; Chen, S.; Leung, A. K.; Leaver, T. J.; Wild, A. W.; Lee, J. B.; Taylor, R. J.; Tam, Y. K.; Hansen, C. L.; Cullis, P. R. Microfluidic Synthesis of Highly Potent Limit-Size Lipid Nanoparticles for *in vivo* Delivery of siRNA. *Mol. Ther.–Nucleic Acids* **2012**, *1*, e37.

(8) Leung, A. K.; Hafez, I. M.; Baoukina, S.; Belliveau, N. M.; Zhigaltsev, I. V.; Afshinmanesh, E.; Tieleman, D. P.; Hansen, C. L.; Hope, M. J.; Cullis, P. R. Lipid Nanoparticles Containing siRNA Synthesized by Microfluidic Mixing Exhibit an Electron-Dense Nanostructured Core. *J. Phys. Chem. C* **2012**, *116*, 18440−18450.

(9) Wan, C.; Allen, T. M.; Cullis, P. R. Lipid Nanoparticle Delivery Systems for siRNA-Based Therapeutics. *Drug Delivery Transl. Res.* **2014**, *4*, 74−83.

(10) Leung, A. K.; Tam, Y. Y.; Chen, S.; Hafez, I. M.; Cullis, P. R. Microfluidic Mixing: A General Method for Encapsulating Macromolecules in Lipid Nanoparticle Systems. *J. Phys. Chem. B* **2015**, *119*, 8698−706.

(11) Viger-Gravel, J.; Schantz, A.; Pinon, A. C.; Rossini, A. J.; Schantz, S.; Emsley, L. Structure of Lipid Nanoparticles Containing siRNA or mRNA by Dynamic Nuclear Polarization-Enhanced NMR Spectroscopy. *J. Phys. Chem. B* **2018**, *122*, 2073−2081.

(12) Hirota, S.; de Ilarduya, C. T.; Barron, L. G.; Szoka, F. C., Jr. Simple Mixing Device to Reproducibly Prepare Cationic Lipid-DNA Complexes (Lipoplexes). *Biotechniques* **1999**, *27*, 286−90.

(13) Jeffs, L. B.; Palmer, L. R.; Ambegia, E. G.; Giesbrecht, C.; Ewanick, S.; MacLachlan, I. A Scalable, Extrusion-Free Method for Efficient Liposomal Encapsulation of Plasmid DNA. *Pharm. Res.* **2005**, *22*, 362−372.

(14) Zhigaltsev, I. V.; Belliveau, N.; Hafez, I.; Leung, A. K.; Huft, J.; Hansen, C.; Cullis, P. R. Bottom-up Design and Synthesis of Limit Size Lipid Nanoparticle Systems with Aqueous and Triglyceride Cores Using Millisecond Microfluidic Mixing. *Langmuir* **2012**, *28*, 3633−40.

(15) Kulkarni, J. A.; Tam, Y. Y. C.; Chen, S.; Tam, Y. K.; Zaifman, J.; Cullis, P. R.; Biswas, S. Rapid Synthesis of Lipid Nanoparticles Containing Hydrophobic Inorganic Nanoparticles. *Nanoscale* **2017**, *9*, 13600−13609.




DOI: 10.1021/acsnano.8b01516
*ACS Nano* XXXX, XXX, XXX−XXX

(16) Heyes, J.; Palmer, L.; Bremner, K.; MacLachlan, I. Cationic Lipid Saturation Influences Intracellular Delivery of Encapsulated Nucleic Acids. *J. Controlled Release* **2005**, *107*, 276−87.
(17) Chen, S.; Tam, Y. Y. C.; Lin, P. J. C.; Sung, M. M. H.; Tam, Y. K.; Cullis, P. R. Influence of Particle Size on the *in vivo* Potency of Lipid Nanoparticle Formulations of siRNA. *J. Controlled Release* **2016**, *235*, 236−244.
(18) Hamilton, J. A.; Small, D. M. Solubilization and Localization of Triolein in Phosphatidylcholine Bilayers: A 13c Nmr Study. *Proc. Natl. Acad. Sci. U. S. A.* **1981**, *78*, 6878−82.
(19) Maurer, N.; Wong, K. F.; Stark, H.; Louie, L.; McIntosh, D.; Wong, T.; Scherrer, P.; Semple, S. C.; Cullis, P. R. Spontaneous Entrapment of Polynucleotides Upon Electrostatic Interaction with Ethanol-Destabilized Cationic Liposomes. *Biophys. J.* **2001**, *80*, 2310−26.
(20) Semple, S. C.; Klimuk, S. K.; Harasym, T. O.; Dos Santos, N.; Ansell, S. M.; Wong, K. F.; Maurer, N.; Stark, H.; Cullis, P. R.; Hope, M. J.; Scherrer, P. Efficient Encapsulation of Antisense Oligonucleotides in Lipid Vesicles Using Ionizable Aminolipids: Formation of Novel Small Multilamellar Vesicle Structures. *Biochim. Biophys. Acta, Biomembr.* **2001**, *1510*, 152−166.
(21) Angelov, B.; Garamus, V. M.; Drechsler, M.; Angelova, A. Structural Analysis of Nanoparticulate Carriers for Encapsulation of Macromolecular Drugs. *J. Mol. Liq.* **2017**, *235*, 83−89.
(22) Angelov, B.; Angelova, A.; Drechsler, M.; Garamus, V. M.; Mutafchieva, R.; Lesieur, S. Identification of Large Channels in Cationic PEGylated Cubosome Nanoparticles by Synchrotron Radiation SAXS and Cryo-Tem Imaging. *Soft Matter* **2015**, *11*, 3686−3692.
(23) Chen, S.; Tam, Y. Y.; Lin, P. J.; Leung, A. K.; Tam, Y. K.; Cullis, P. R. Development of Lipid Nanoparticle Formulations of siRNA for Hepatocyte Gene Silencing Following Subcutaneous Administration. *J. Controlled Release* **2014**, *196*, 106−12.
(24) Akinc, A.; Zumbuehl, A.; Goldberg, M.; Leshchiner, E. S.; Busini, V.; Hossain, N.; Bacallado, S. A.; Nguyen, D. N.; Fuller, J.; Alvarez, R.; Borodovsky, A.; Borland, T.; Constien, R.; de Fougerolles, A.; Dorkin, J. R.; Narayanannair Jayaprakash, K.; Jayaraman, M.; John, M.; Koteliansky, V.; Manoharan, M.; et al. A Combinatorial Library of Lipid-Like Materials for Delivery of RNAi Therapeutics. *Nat. Biotechnol.* **2008**, *26*, 561−9.
(25) Basha, G.; Ordobadi, M.; Scott, W. R.; Cottle, A.; Liu, Y.; Wang, H.; Cullis, P. R. Lipid Nanoparticle Delivery of siRNA to Osteocytes Leads to Effective Silencing of *Sost* and Inhibition of Sclerostin *in vivo*. *Mol. Ther.–Nucleic Acids* **2016**, *5*, e363.



DOI: 10.1021/acsnano.8b01516
*ACS Nano* XXXX, XXX, XXX−XXX